Tubulation by amphiphysin requires concentration-dependent switching from wedging to scaffolding

J. Mario Isas[1,*] and Mark R. Ambroso[1,*], Prabhavati B. Hegde[1], Jennifer Langen[2], Ralf Langen[1,¥]

[1]Zilkha Neurogenetic Institute, University of Southern California, Los Angeles, California 90033, USA.
[2]Department of Biological Sciences, University of Southern California, Los Angeles, CA 90089-2910, USA.

[¥]Corresponding Author: Ralf Langen, Zilkha Neurogenetic Institute, 1501 San Pablo St., 121 ZNI, Los Angeles, CA 90033. Tel.: 323-442-1323 Fax: 323-442-4404. Email langen@usc.edu

Supplemental Data

Figure S1, related to Figure 1.

EPR continuous wave spectra, as well as NiEDDA and O_2 accessibilities, of spin labeled derivatives of amphiphysin bound to 100 nm vesicles.

(A) Continuous wave (CW) EPR spectra of spin labeled amphiphysin containing spin label R1 at position 13 in solution (black) and bound to vesicles (red). Sharp spectral lines indicate high spin label mobility in solution. The broadened spectra for the vesicle bound form indicate reduced mobility. All other N-terminal labeling sites had similar spectra in solution indicating an unfolded structure.

(B) The CW EPR spectra of N-terminally spin labeled derivatives of amphiphysin when bound to vesicles.

(C) The N-terminal amino acid sequence of *Drosophila melanogaster* amphiphysin.

(D) Accessibility to oxygen (ΠO_2) and NiEDDA (ΠNiEDDA) as function of labeling position for vesicle bound amphiphysin. The periodicity in the respective accessibilities is indicative of α-helical secondary conformation (Hubbell et al., 1998) and the out-of phase periodicity indicates that this helical structure is amphipathic.

(E) Lipids containing spin labels at known bilayer immersion depths (Bretscher et al., 2008; Dalton et al., 1987) were analyzed for accessibility to O_2 and NiEDDA in vesicles bound by non-spin labeled amphiphysin. These values were used to calibrate (Φ) with respect to membrane immersion depth (d) in Å (Altenbach et al., 1994). The values were fit to a hyperbolic tangent function (black line), $\Phi = A \tanh[B(x-C)] + D$, as previously described (Frazier et al., 2002), where A= 2.7, B= 0.08, C= 14, D= 2.5, and x is depth given in Å. Error bars represent SD, n = at least three independent experiments.

(F-G) CW EPR spectra of vesicle bound (red) and soluble (black) amphiphysin spin labeled in the BAR domain at the indicated positions, which are also shown in Figure 1A. High or low spectral amplitudes were rescaled using the indicated scaling factor (e.g., "2x") for space considerations. Scan width is 100 gauss.

Figure S2, related to Figure 2.

EPR continuous wave spectra, as well as NiEDDA and O_2 accessibilities, of spin labeled derivatives in the N-terminus of amphiphysin bound to lipid tubes.

(A) CW EPR spectra of amphiphysin R1-labeled at position 13 in solution (black) and bound to tubes (red).

(B) CW EPR spectra of tube bound amphiphysin labeled with R1 at the indicated N-terminal sites.

(C) Accessibility to O_2 (ΠO_2) and NiEDDA (ΠNiEDDA) as a function of labeling position for tube bound amphiphysin.

(D) Accessibility to O_2 and NiEDDA of spin labeled lipids in tubes formed by non-spin labeled amphiphysin were used to calibrate Φ with respect to immersion depth (Altenbach et al., 1994). The values were fit to a hyperbolic tangent function (black line), $\Phi = A \tanh[B(x-C)] + D$, where A= 3.1, B= 0.04, C= 10, D= 1.2, and x is depth given in Å. Error bars represent SD, n = at least three independent experiments.

Figure S3, related to Figure 3.

Spin label mobility and accessibility for spin labeled amphiphysin bound to tubes or to vesicles.

(A-B) CW EPR spectra of amphiphysin derivatives spin labeled in the BAR domain at the indicated positions in solution (black) or bound to tubes (red). High or low spectral amplitudes were rescaled using the indicated scaling factor (e.g., "2x") for space considerations. Scan width is 100 gauss.

(C) The percent change in CW EPR spectral central line width for spin labeled amphiphysin derivatives bound to tubes or to vesicles is plotted versus residue number. Derivatives with a percent change in central line width greater than or equal to 10% (dashed line) are highlighted (green).

(D) Crystal structure of drosophilia amphiphysin dimer (pdb, 1URU) indicating spin labeled derivatives with percent central line width changes greater than 10% in green as determined in (C). Residue numbers are given for only one subunit of the dimer.

(E) Plot of ΠO_2 versus ΠNiEDDA for spin labeled sites in the BAR domain bound to tubes (black) or vesicles (red). Prior studies have shown that the accessibilities to O_2 and NiEDDA are linearly related for proteins in solution (Isas et al, 2002). This is indeed the case for all sites in the BAR domain upon vesicle binding, in agreement with the notion that the BAR domain is too far from the membrane to experience enhanced O_2 accessibility. In contrast, accessibility values for several tube bound derivatives do not fall into the same diagonal region delineated by the dashed lines. A number of sites fall below the dashed line as a consequence of enhanced O_2 accessibility due to membrane proximity. The plot also shows that the enhanced Φ values in Figure 3A are not due to the "excluded volume effect". In very rare cases, enhanced Φ values can be the consequences of the "excluded volume effect" in exceedingly immobilized regions (Isas et al., 2002). In such a scenario, sites may be very inaccessible to both O_2 and NiEDDA, but due to its smaller size, accessibility to O_2 is non-zero while accessibility to the larger molecule of NiEDDA is near zero. The plot indicates that this is not the case here.

Table S1, related to Figures 1 and 3.

O_2 and NiEDDA accessibilities for all of the spin labeled amphiphysin derivatives in vesicle or tube bound states. Values are the average of at least 3 independent measurements.

Figure S1

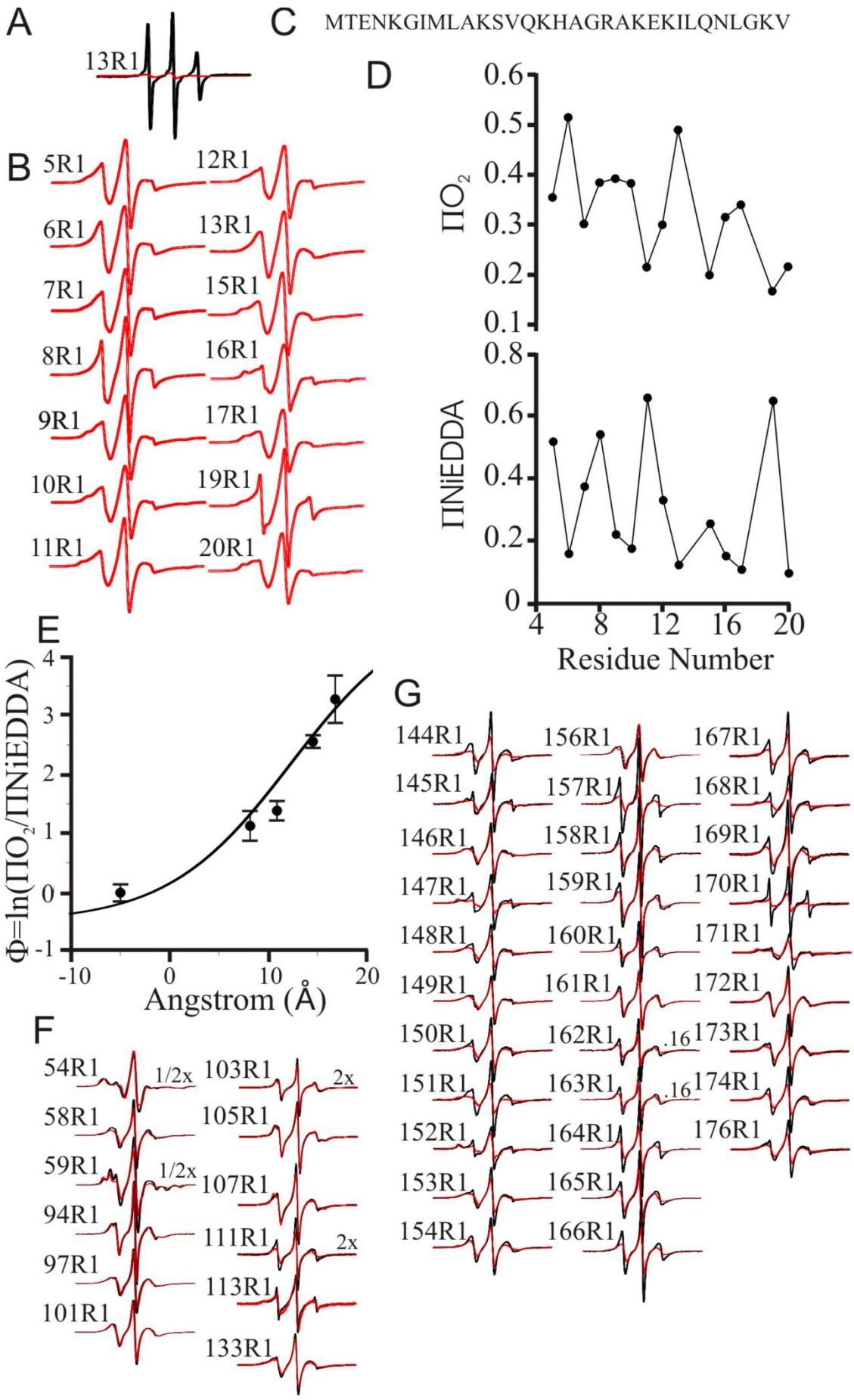
A
13R1
B
5R1
6R1
7R1
8R1
9R1
10R1
11R1
12R1
13R1
15R1
16R1
17R1
19R1
20R1
C
MTENKGIMLAKSVQKHAGRAKEKILQNLGKV
D
ΠO2
ΠNiEDDA
Residue Number
E
Φ=ln(ΠO2/ΠNiEDDA)
Angstrom (Å)
F
54R1
58R1
59R1
94R1
97R1
101R1
103R1
105R1
107R1
111R1
113R1
133R1
1/2x
2x
G
144R1
145R1
146R1
147R1
148R1
149R1
150R1
151R1
152R1
153R1
154R1
156R1
157R1
158R1
159R1
160R1
161R1
162R1
163R1
164R1
165R1
166R1
167R1
168R1
169R1
170R1
171R1
172R1
173R1
174R1
176R1
.16

Figure S2

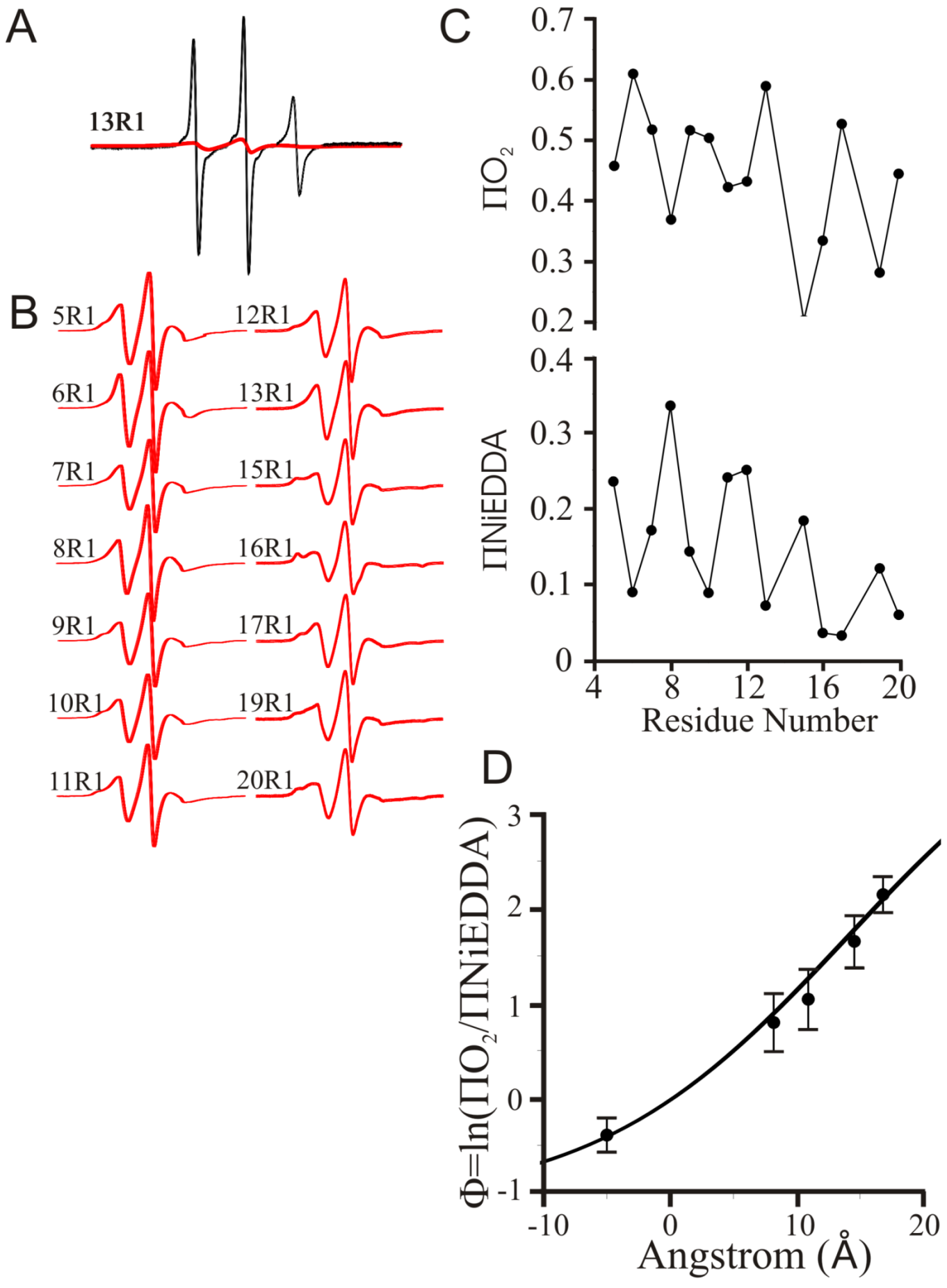
A
13R1
B
5R1
12R1
6R1
13R1
7R1
15R1
8R1
16R1
9R1
17R1
10R1
19R1
11R1
20R1
C
ΠO2
0.7
0.6
0.5
0.4
0.3
0.2
ΠNiEDDA
0.4
0.3
0.2
0.1
0
4
8
12
16
20
Residue Number
D
Φ=ln(ΠO2/ΠNiEDDA)
3
2
1
0
-1
-10
0
10
20
Angstrom (Å)

Figure S3

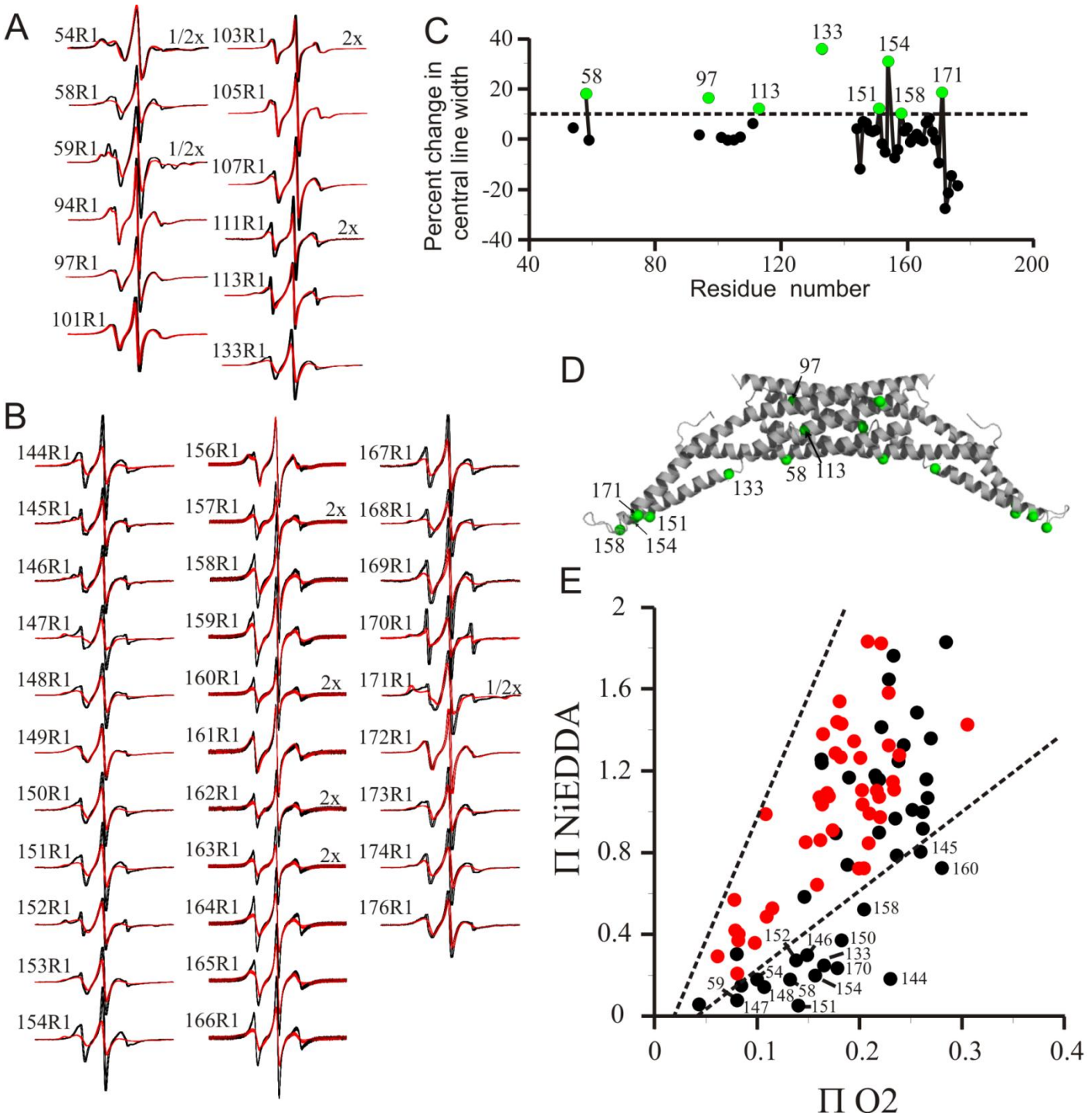
A
54R1
1/2x
103R1
2x
58R1
105R1
59R1
1/2x
107R1
94R1
111R1
2x
97R1
113R1
101R1
133R1
B
144R1
156R1
167R1
145R1
157R1
2x
168R1
146R1
158R1
169R1
147R1
159R1
170R1
148R1
160R1
2x
171R1
1/2x
149R1
161R1
172R1
150R1
162R1
2x
173R1
151R1
163R1
2x
174R1
152R1
164R1
176R1
153R1
165R1
154R1
166R1
C
Percent change in central line width
40
20
0
-20
-40
40
80
120
160
200
Residue number
58
97
113
133
154
151
158
171
D
97
58
113
133
171
151
158
154
E
Π NiEDDA
Π O2
2
1.6
1.2
0.8
0.4
0
0
0.1
0.2
0.3
0.4
145
160
158
152
146
150
133
170
54
144
59
148
58
154
147
151

Table S1

Spin labeled derivative	Tube-bound		Vesicle-bound	
	ΠO_2	ΠNiEDDA	ΠO_2	ΠNiEDDA
5	0.46	0.23	0.36	0.52
6	0.61	0.09	0.52	0.16
7	0.52	0.17	0.30	0.37
8	0.37	0.33	0.39	0.54
9	0.52	0.09	0.39	0.18
10	0.50	0.09	0.39	0.18
11	0.42	0.24	0.22	0.66
12	0.43	0.25	0.30	0.33
13	0.59	0.07	0.49	0.12
15	0.20	0.18	0.20	0.26
16	0.33	0.04	0.32	0.15
17	0.53	0.03	0.34	0.11
19	0.28	0.12	0.17	0.65
20	0.45	0.06	0.22	0.10
54	0.10	0.18	0.08	0.40
58	0.13	0.18	0.18	1.29
59	0.08	0.15	0.08	0.42
94	0.27	1.36	0.22	1.10
97	0.19	1.17	0.31	1.43
101	0.27	1.07	0.23	1.11
103	0.16	1.25	0.16	1.03
105	0.22	1.16	0.21	0.99
107	0.22	1.41	0.23	1.15
111	0.23	1.65	0.18	1.43
113	0.24	1.25	0.21	0.85
133	0.17	0.25	0.17	0.91
144	0.23	0.18	0.11	0.49
145	0.26	0.80	0.20	0.72
146	0.15	0.30	0.16	0.64
147	0.08	0.08	0.08	0.21
148	0.11	0.14	0.10	0.36

Table S1 (continued)

149	0.19	0.74	0.18	1.44
150	0.18	0.37	0.16	0.86
151	0.14	0.05	0.08	0.37
152	0.14	0.27	0.11	0.53
153	0.24	0.79	0.20	0.72
154	0.16	0.20	0.15	0.85
156	0.26	1.00	0.20	1.04
157	0.23	0.97	0.21	1.83
158	0.20	0.52	0.18	1.27
159	0.25	1.01	0.22	1.07
160	0.28	0.72	0.22	0.97
161	0.27	1.16	0.22	1.82
162	0.26	0.92	0.23	1.58
163	0.24	1.32	0.24	1.28
164	0.22	0.90	0.20	1.26
165	0.26	1.48	0.18	1.54
166	0.16	1.24	0.19	1.34
167	0.15	0.58	0.16	1.07
168	0.22	1.18	0.20	1.10
169	0.23	1.76	0.23	1.32
170	0.18	0.24	0.11	0.99
171	0.04	0.06	0.06	0.29
172	0.28	1.83	0.17	1.07
173	0.18	0.89	0.16	1.38
174	0.08	0.30	0.08	0.57
176	0.22	1.16	0.17	1.09

Supplemental references:

Altenbach, C., Greenhalgh, D.A., Khorana, H.G., and Hubbell, W.L. (1994). A collision gradient method to determine the immersion depth of nitroxides in lipid bilayers: application to spin-labeled mutants of bacteriorhodopsin. Proc. Natl. Acad. Sci. *91*, 1667–1671.

Bretscher, L.E., Buchaklian, A.H., and Klug, C.S. (2008). Spin-labeled lipid A. Anal. Biochem. *382*, 129–131.

Dalton, L.A., McIntyre, J.O., and Fleischer, S. (1987). Distance estimate of the active center of D-beta-hydroxybutyrate dehydrogenase from the membrane surface. Biochemistry *26*, 2117–2130.

Frazier, A.A., Roller, C.R., Havelka, J.J., Hinderliter, A., and Cafiso, D.S. (2003). Membrane-Bound Orientation and Position of the Synaptotagmin I C2A Domain by Site-Directed Spin Labeling. Biochemistry *42*, 96–105.

Hubbell, W.L., Gross, A., Langen, R., and Lietzow, M.A. (1998). Recent advances in site-directed spin labeling of proteins. Curr. Opin. Struct. Biol. *8*, 649–656.

Isas, J.M., Langen, R., Haigler, H.T., and Hubbell, W.L. (2002). Structure and Dynamics of a Helical Hairpin and Loop Region in Annexin 12: A Site-Directed Spin Labeling Study. Biochemistry *41*, 1464–1473.